

## Micro-seismic monitoring in mines based on cross wavelet transform

Linqi Huang<sup>\*1,2</sup>, Hong Hao<sup>2</sup>, Xibing Li<sup>1</sup> and Jun Li<sup>2</sup>

<sup>1</sup>*School of Resources and Safety Engineering, Central South University, Changsha, Hunan 410083, China*

<sup>2</sup>*Centre for Infrastructural Monitoring and Protection, School of Civil and Mechanical Engineering, Curtin University, Bentley, WA6102, Australia*

*(Received April 1, 2016, Revised May 10, 2016, Accepted June 26, 2016)*

**Abstract.** Time Delay of Arrival (TDOA) estimation methods based on correlation function analysis play an important role in the micro-seismic event monitoring. It makes full use of the similarity in the recorded signals that are from the same source. However, those methods are subjected to the noise effect, particularly when the global similarity of the signals is low. This paper proposes a new approach for micro-seismic monitoring based on cross wavelet transform. The cross wavelet transform is utilized to analyse the measured signals under micro-seismic events, and the cross wavelet power spectrum is used to measure the similarity of two signals in a multi-scale dimension and subsequently identify TDOA. The offset time instant associated with the maximum cross wavelet transform spectrum power is identified as TDOA, and then the location of micro-seismic event can be identified. Individual and statistical identification tests are performed with measurement data from an in-field mine. Experimental studies demonstrate that the proposed approach significantly improves the robustness and accuracy of micro-seismic source locating in mines compared to several existing methods, such as the cross-correlation, multi-correlation, STA/LTA and Kurtosis methods.

**Keywords:** micro-seismic monitoring; source location; TDOA; cross wavelet transform

### 1. Introduction

Since underground mines continue to evolve at deeper levels with an increasing strength of mining activities, a large number of mines all over the world have suffered adverse impacts of micro-seismic vibrations. Most micro-seismic activities in mines cannot be felt distinctively. However, they actually occur widely and frequently, associated closely with the mining engineering activities and the surrounding environment. They may result in the significant economic losses, engineering structural damage, and even the gas and coal dust explosion (Chalmers 2013, Dong *et al.* 2014, Zhao *et al.* 2015, Li *et al.* 2015a). The successful detection and location prediction of micro-seismic activities are of vital importance to ensure the normal operation and safety of mines.

Micro-seismic monitoring in mines is a common way to investigate and control mine disasters. It could predict the possible location of mine disasters by monitoring the vibration of mines in real

---

\*Corresponding author, E-mail: [linqi.huang@curtin.edu.au](mailto:linqi.huang@curtin.edu.au), [huanglinqi1211@gmail.com](mailto:huanglinqi1211@gmail.com)

time with arranged sensors (Li *et al.* 2015b, Li *et al.* 2016). Among the many micro-seismic source locating methods, the method based on Time Delay of Arrival (TDOA) is the most popular one. The main idea and procedure behind these methods are that the location of the micro-seismic event is determined through analysing the delay in arrival times of recorded seismic waves at spatial sensor locations and correlating these delay times with the wave propagation velocity and the spatial coordinates of the sensors. Therefore determining the accurate arrival time at each sensor and the time delay between seismic wave arrivals at multi sensors are essential for reliably locating the micro-seismic source.

In actual in-situ micro-seismic monitoring, it is often impossible to obtain the precise location of every micro-seismic event because there are numerous micro-seismic event records in every minute and usually there is no continuous service to immediately examine the site condition and determine the true source location. The general engineering practise to define the reference location of the micro-seismic event is based on the calculation with the assumed speed model and calculated TDOA, which is traditionally determined by the experienced in-situ experts and analyst (Saragiotis *et al.* 2004).

On the other hand, the automatic methods for identifying TDOA become popular in recent decades. There are two different categories of automatic methods, namely, the absolute method and the relative method. The absolute method is based on picking up the absolute arrival time of the first arrival wave from different sensors. TDOA is obtained as the difference between the absolute arrival time instants. To reliably pick up the arrival time instants from recorded noisy signals, various techniques have been proposed. The commonly used methods include the neural network algorithm (McCormack *et al.* 1993, Yuksel and Yazar 2015), the fractal dimensions techniques (Boschetti *et al.* 1996, Jiao and Moon 2012), the short time average over long-time average ratio (STA/LTA) method, the modified energy ratio technique (Wong *et al.* 2009, Munro 2004, Han *et al.* 2010), etc. The reliability of these approaches is dependent on the accuracy of picking up the arrival time instants, sensor network geometry, and the wave propagation velocity (Pavlis 1986, Gomberg *et al.* 1990).

The relative methods do not require the detection of the absolute arrival time of measured waves. TDOA is obtained based on the similarity of two signals that are from the same or proximal source. The relative method is developed firstly in the field of analyzing the acoustic wave source (Knapp and Carter 1976). In a subsequent study that characterized the similarity of the waveforms by cross-correlation function, it was found that when the correlation value is the maximum, the time offset is most likely the time delay between the two analysed wave records (Carter 1987). The latter study is probably the first time TDOA is calculated by the relative method. It was called time delay estimation (TDE) at that time. In the recent two decades, the relative method has been applied widely in different areas (Jiang *et al.* 2013, Zhong *et al.* 2014, Nistor and Buda 2015, Huang and Benesty 2007), such as geophysics, seismology, acoustic, satellite navigation, radio, radar, sonar, and ultrasonics. Most of the relative methods for identifying TDOA, such as the double-difference algorithm (DDA) (Waldhauser and Ellsworth 2000), the generalized cross-correlation (GCC) (Knapp and Carter 1976) and generalized cross correlation with phase transform (GCC-PHAT) (Kwon *et al.* 2010), evaluate the similarity of two signals by means of the correlation function or cross covariance. The difference in these methods lies on adding up the different filtering processing to improve the location identification accuracy, such as Fourier technique (Knapp and Carter 1976, Carter 1987, Huang and Jacob 2001), autocorrelation filter (He and Zhao 2010) and wavelet technique (Kwon and Chan 1998, Xing *et al.* 2002, Law *et al.* 2013). The combination of cross-correlation function and Fourier transform

allows the analysis of the signals in both the frequency and time domains (Knapp and Carter 1976, Carter 1987, Huang and Benesty 2007). This approach reduces the source locating error to a certain extent but it can only perform the analysis in the global scale. This limits the accuracy of the method in locating the micro-seismic source because one of the most obvious characteristics of micro-seismic signals is the non-stationarity and randomness (Xing *et al.* 2002, Correig and Urquizú 2002, Sobolev *et al.* 2005). The multiple correlation method reduces the influence of noise to some extent by using the autocorrelation for computing the cross-correlation. To improve the accuracy in locating the micro-seismic source, the wavelet transform correlation based method for identifying the TDOA was proposed. The approach is a kind of multi-scale analysis approach (Kwon and Chan 1998). Moreover, the combined method could also analyse the signals in both the frequency and time domains. Wang and Chu (2001) decomposed the original acoustic signal into a series of time-domain signals, and then calculated the cross-correlation between the decomposed signals. This method analysed the signals in a specific frequency band, but the time-frequency information has not been fully used in the similarity analysis for the determination of the rubbing locations.

TDOA estimation methods based on correlation function analysis play an important role in the micro-seismic event monitoring, which make use of the similarity in the recorded signals that are from the same source. However, those methods are subjected to the noise effect, particularly when the global similarity of the signals is low. This paper proposes a new approach for micro-seismic monitoring based on cross wavelet transform. The cross wavelet transform is utilized to analyse the measured signals under micro-seismic events, and the cross wavelet power spectrum is used to measure the similarity of two signals in a multi-scale dimension and subsequently identify TDOA. The offset time instant associated with the maximum cross wavelet transform spectrum power is identified as TDOA, and then the location of micro-seismic events can be identified. Individual and statistical identification tests are performed with measurement data from an in-field mine. Identification results demonstrate and compare the robustness and accuracy of the proposed approach in locating micro-seismic source in mines with several existing methods such as, cross-correlation, multi-correlation, STA/LTA and Kurtosis methods.

## 2. Theoretical background of traditional methods

P-wave and S-wave are body waves travelling within the Earth. The difference in arrival time of waves can be used to locate a seismic event like an earthquake. P-wave has the highest velocity and is therefore the first wave to be recorded. Therefore, P-wave is normally used for micro-seismic monitoring in mines. Assuming that the travelling speed of the P-wave due to the micro-seismic event is constant in a homogeneous isotropic medium, Eq. (1) can be obtained for each sensor based on the fundamental theory of wave propagation

$$\sqrt{(x_i - x)^2 + (y_i - y)^2 + (z_i - z)^2} = v(t_i - t) \quad (1)$$

where  $(x_i, y_i, z_i)$  and  $(x, y, z)$  denote the spatial coordinates of the  $i^{\text{th}}$  sensor and the micro-seismic source, respectively;  $v$  denotes the travelling speed of the P-wave;  $t$  and  $t_i$  respectively represent the time instants of the micro-seismic event and the arrival time of the P-wave at the  $i^{\text{th}}$  sensor location.

Subtracting two equations corresponding to sensors  $i$  and  $j$  in the form of Eq. (1), Eq. (2) is

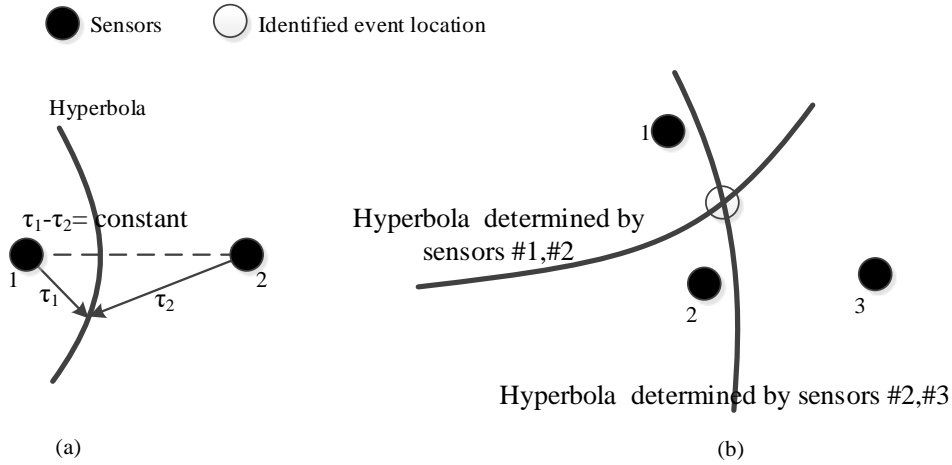


Fig. 1 The schematic illustration (a) a hyperbola determined by two sensors and their TDOA (b) micro-seismic event location identification with TDOA in a planar space

obtained as

$$\sqrt{(x_i - x)^2 + (y_i - y)^2 + (z_i - z)^2} - \sqrt{(x_j - x)^2 + (y_j - y)^2 + (z_j - z)^2} = v(t_i - t_j) \quad (2)$$

The propagation speed of the P-wave and the spatial coordinates of those two sensors are usually available in practice. The most critical thing in solving Eq. (2) for determination of the seismic source coordinates is the accuracy of estimating the arrival time difference ( $t_i - t_j$ ), which is TDOA. From Eq. (2), a hyperbola trajectory can be obtained with the two sensor locations 1, 2 as the foci, as shown in Fig. 1(a). The source location of the micro-seismic event must locate on the hyperbolic trajectory so it can be identified by examining the intersection of several hyperbolas. In planar space, at least two hyperbolas are needed to determine the source location, as shown in Fig. 1(b). In the same way, at least three hyperbolas are required to locate the micro-seismic event location accurately in a three-dimensional space. In other words, to determine the three unknowns  $x$ ,  $y$ , and  $z$  in the parabola equation, three independent equations are needed to find the solution. Some traditional and typical methods from existing studies will be briefly reviewed here.

### 2.1 Cross-correlation Method

The cross-correlation method is suitable for identifying and locating the micro-seismic event from multi-channel sensor responses. The arrival time instants of both the P wave and S wave can be picked up respectively and successively. Cross-correlation function is a real function, which could be positive and negative, and can be used to measure the similarity between two signals (Liu *et al.* 2009, Zhang *et al.* 2013).

The cross-correlation of two random variables  $x$  and  $y$  is defined as

$$R_{xy}(\tau) = E\{x(i)y(i + \tau)\} \quad (3)$$

where  $E$  denotes the expectation in mathematics. For two signals  $x(i)$  and  $y(i)$  ( $i=1, 2, \dots, n$ ), with  $n$

equal to the number of data points in the signals, the above formula can be expressed as follows

$$\hat{R}_{xy}(\tau) = \sum_{i=1}^n (x(i)y(i+\tau)/n) \quad (4)$$

Assuming that  $s(i)$  is the true signal from the micro-seismic event, and  $x(i)$  and  $y(i)$  are the measured signals at the  $i^{\text{th}}$  and  $j^{\text{th}}$  sensors respectively,  $x(i)$  and  $y(i)$  inevitably involve noises and can be expressed by adding  $s(i)$  with noisy signals  $w_1(i)$  and  $w_2(i)$  respectively as

$$x(i) = \alpha s(i - \tau_1) + w_1(i) \quad (5)$$

$$y(i) = \beta s(i - \tau_2) + w_2(i) \quad (6)$$

where  $\alpha$  and  $\beta$  are two constants related to the wave propagation to those two sensors,  $\tau_1$  and  $\tau_2$  are the delayed time instants that the wave transmits from the source to those two sensor locations respectively.

Based on the calculation of cross-correlation as shown in Eq. (4), the cross-correlation function between  $x(i)$  and  $y(i)$  can be simplified as follows

$$R_{xy}(\tau) = \alpha\beta E(s(i) \cdot s(i - \tau - (\tau_1 - \tau_2))) \quad (7)$$

$R_{xy}(\tau)$  would reach the maximum value when  $\tau = \tau_1 - \tau_2$ , which means that the delay corresponding to the maximum value in the cross-correlation function is the theoretical TDOA between those two sensors.

## 2.2 Multi-correlation method

The above cross-correlation method is not necessarily suitable for non-stationary signals, and the noise effect may have a significant influence on the identification accuracy. To overcome this, the auto-correlation of signals can be calculated first before obtaining the cross-correlation function to suppress the high-frequency noise components in the signals. Through this the white noise effect could be eliminated, and the signal-to-noise ratio is improved, which also improves the estimation of time delay.

Considering two signals,  $x(i)$  and  $y(i)$  as mentioned in Eqs. (5)-(6), the auto-correlation function of  $x(i)$  and the cross-correlation function of  $x(i)$  and  $y(i)$ , can be expressed respectively as

$$R_{xx}(k) = \sum_{i=1}^n (x(i)x(i+k)/n) \quad (8)$$

$$R_{xy}(k) = \sum_{i=1}^n (x(i)y(i+k)/n) \quad (9)$$

Since micro-seismic signal  $s(i)$  is uncorrelated to the noise signal  $w(i)$ , their cross-correlation coefficient is 0. If we define

$$r(j) = \sum_{i=1}^n (s(i)s(i+j)/n) \quad (10)$$

then the following formula can be obtained

$$R_{xx}(k) = \sum_{i=1}^n (s(i)s(i+k)/n) + \sum_{i=1}^n (w(i)w(i+k)/n) = r(i+k) + \sum_{i=1}^n (w(i)w(i+k)/n) \quad (11)$$

$$R_{xy}(k) = \sum_{i=1}^n (s(i)s(i-\tau+k)/n) + \sum_{i=1}^n (w(i)w(i+k)/n) = r(i-\tau+k) + \sum_{i=1}^n (w(i)w(i+k)/n) \quad (12)$$

It can be derived from Eqs. (11) and (12), the delay between  $R_{xx}$  and  $R_{xy}$  is  $\tau$ . Since the autocorrelation of the white noise signal  $w(i)$  is 0, the signal-to-noise ratio of auto-correlation function  $R_{xx}(k)$  and cross-correlation function  $R_{xy}(k)$  is higher than the original signals  $x(i)$  and  $y(i)$  respectively, which makes the estimation of TDOA more accurate.

### 2.3 STA/LTA method

The above-mentioned methods estimate TDOA with a relative approach, which means that the relative difference between the arrival time instants at two sensors is calculated. Short Term Averaging/Long Term Averaging (STA/LTA) method belongs to the category of absolute methods, where the absolute arrival time of P-wave is identified and TDOA between the arrival times at different sensors is obtained by comparing their absolute arrival time instants. STA/LTA algorithm is one of the most widely used methods in this category (Earle and Shearer 1994). Two different moving time windows along the time axis (one short term and the other long term window) are defined, and the corresponding power of the signal within these two time windows are calculated to determine the arrival time instant of the micro-seismic event by identifying the maximum value in the power ratio of STA/LTA. STA and LTA denote the energies of the measured signal due to the micro-seismic events and background signals including noise effect, respectively. If the micro-seismic signal is  $s(i)$ , then STA/LTA at the time instant  $\tau$  can be expressed as

$$\frac{STA}{LTA}(\tau) = \frac{\sum_{i=\tau-N_{STA}}^{\tau} CF(s(i)) / N_{STA}}{\sum_{i=\tau-N_{LTA}}^{\tau} CF(s(i)) / N_{LTA}} \quad (13)$$

in which  $CF$  is a feature function, which characterizes the amplitude or phase of measured signals due to the micro-seismic event, and is usually defined as the absolute value, square or the first derivative, etc. The data points in the long term and short term windows are  $N_{LTA}$  and  $N_{STA}$ , respectively. The merit of this method is the high efficiency, but the selection of the length of the time window may affect the estimation accuracy greatly, especially when the noise effect is significant.

### 2.4 Kurtosis method

Kurtosis is a measure of the “tailedness” of the probability distribution of a real-valued random variable, which is similar to the concept of skewness. It is a descriptor of the steepness of a probability distribution and can be expressed as the fourth standardized moment as follows

$$Kurt(x) = \frac{\mu_4(x)}{\sigma(x)^4} = \frac{E[(x - \mu)^4]}{(E[(x - \mu)^2])^2} \quad (14)$$

in which  $\mu(x)$  and  $\sigma(x)$  are the mean and standard deviation of  $x$  respectively.

The arrival time of the micro-seismic event can be obtained by calculating a series of Kurtosis values along a sliding time window of the signal and picking up the time instant corresponding to the maximum Kurtosis value (Saragiotis *et al.* 2002). The disadvantage of this method is that the detection is vulnerable to the noise and the selection of the time window. Kurtosis method is a kind of absolute method.

Among the above four existing methods, the first two methods are relative methods, where it is not necessary to identify the absolute arrival time of the micro-seismic wave. TDOA can be obtained by the maximum value of the cross correlation function of two signals from the same source in these two methods. The latter two are absolute methods, where TDOA is calculated between the picked absolutely arrival time instants of P wave in the measured signals from sensors (Aminzadeh *et al.* 2011).

### 3. Developed approach based on cross wavelet transform

#### 3.1 Theoretical development

In this study, the source location of a micro-seismic event is identified based on the cross wavelet transform. The theoretical background and development of the proposed approach are presented here.

For a discrete signal  $x(t)$  ( $t=1, 2, \dots, N$ ), the continuous wavelet transform with uniform time steps  $\delta t$  can be expressed as the convolution of  $x(n)$  with the scaled and normalized mother wavelet function

$$WT^x(u, s) = \sqrt{\frac{\delta t}{s}} \sum_{t=1}^N x(t) \psi_0 \left[ (t - u) \frac{\delta t}{s} \right] \quad (15)$$

in which  $u$  is the translation parameter,  $s$  is the scale parameter. The mother wavelet function is defined as Morlet wavelet because of its excellent balance between the time and frequency localization especially for characteristic extraction (Grinsted *et al.* 2004). The Morlet wavelet can be expressed as

$$\psi_0(\eta) = \pi^{-1/4} e^{i\omega_0\eta} e^{-\frac{1}{2}\eta^2} \quad (16)$$

where  $\omega_0$  is the wavenumber, in this case,  $\omega_0=6$ .  $\eta$  denotes the non-dimensional time.

The cross wavelet transform of two signals  $x(t)$  and  $y(t)$  ( $t=1, 2, \dots, N$ ) is calculated as

$$WT^{xy}(u, s) = WT^x(u, s) WT^{y*}(u, s) \quad (17)$$

where “\*” indicates the complex conjugation. The cross wavelet spectrum power is defined as  $|WT^{xy}(u, s)|^2$ . The complex argument  $\arg(WT^{xy})$  can be interpreted as the local relative phase

between  $x(t)$  and  $y(t)$  in time frequency space.

When using cross wavelet transform to identify TDOA between two signals  $x_i$  ( $i=1, 2, \dots, N$ ) and  $y_i$  ( $i=1, 2, \dots, N$ ), which are measured by two sensors  $S_1$  and  $S_2$  due to a micro-seismic event, it is assumed that TDOA between signals  $x_i$  and  $y_i$  is of  $k$  sampling steps, i.e.,  $S_2$  detects the P-wave arrival from the micro-seismic event  $k \cdot \delta t$  time instants after  $S_1$  detects it. This means  $x_{i+k}$  (a delay with  $k \cdot \delta t$  time instants on the original signal) and  $y_i$  shall have an excellent similarity, and their cross wavelet spectrum power shall also reach the maximum. Based on this fact, the identification of TDOA between signals  $x_i$  and  $y_i$  is then transformed into an optimization problem to search for the  $k$  sampling steps corresponding to the maximum value of the following objective function,

$$f_{obj} = \max \left| WT^{x_{i+k}y_i}(u, s) \right|^2 \quad (18)$$

Wavelet transform has the edge effect due to the signal discontinuity, which may affect the transformed data. To overcome this, the Cone of Influence (COI) is introduced in the analysis. COI is a region of the wavelet spectrum with its shape similar as a cone. In this study, the area in which the cross wavelet spectrum power caused by a discontinuity at the edge has dropped to  $e^{-2}$  of the value at the edge.

The cross wavelet transform spectrum power within the above selected area and a significance level is calculated. The null hypothesis is defined for the wavelet power spectrum as follows. It is assumed that if a peak in the wavelet power spectrum is significantly above this background spectrum, it can be assumed to be a true feature with a certain percent confidence. For example, “significant at the 5% level” is equivalent to “the 95 confidence level”. The confidence level  $\lambda$  means that when Monte Carlo method is used to calculate the cross wavelet spectrum between

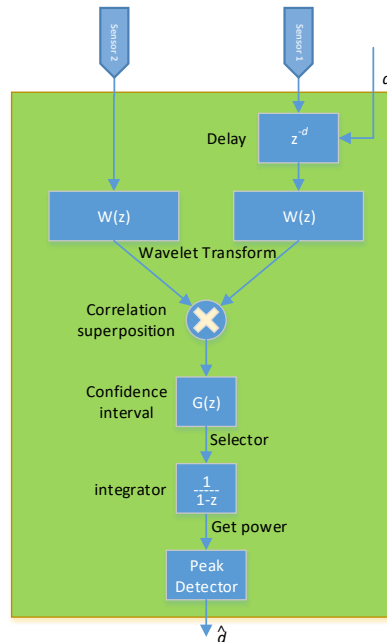


Fig. 2 The flow chart of the proposed approach based on cross wavelet transform



background noises at one point in time-frequency domain, when the possibility of cross-correlation coefficient is less than  $1-\lambda$ , the point belongs to the confidence interval  $\lambda$ . In the following sections, the result of *power* calculated is referred as cross wavelet spectrum power with a high confidence.

### 3.2 Identification procedure

The flowchart of the proposed approach is shown in Fig. 2.

The above flow chart describes how the proposed approach works. Two signals from Sensors 1 and 2 are recorded from the same micro-seismic event source. Various processing steps will be applied, i.e., adding a delay  $d$ , performing wavelet transform, calculating cross wavelet spectrum, applying COI and confidence level to select a high confidence level area of cross wavelet spectrum, calculating the cross wavelet spectrum power and identifying the delay  $\hat{d}$  with the maximum cross wavelet transform spectrum power. TDOA is determined by identifying the specific time step that achieves the maximum cross wavelet spectrum power between two sensor signals. The specific steps are described as follows

Step 1: Two sensor signals  $x(i)$  and  $y(i)$  are acquired from the same micro-seismic event source in mines.

Step 2: After that, a series of time delay  $d_j$  is added to  $x(i)$  respectively. Cross wavelet transform with Morlet wavelet function as previously mentioned is performed for two signals  $x(i+d_i)$  and  $y(i)$ , respectively.

Step 3: Cross wavelet spectrum power is calculated based on the above wavelet transforms in Step 2.

Step 4: After the cross wavelet transform calculation, the selector module is used for selecting the spectrum area  $\Omega$  which has a high confidence. The integrator module is used to calculate the power of spectrum area  $\Omega$ .

Step 5: Lastly, comparing the obtained cross wavelet transform power values from step 4 under different introduced delays  $d_j$  in previous steps, the time delay that leads to the maximum cross wavelet spectrum power is obtained as the TDOA between sensor signals  $x(i)$  and  $y(i)$ . When more than three TDOA from several sensors are determined, the location of the micro-seismic event can be obtained with the available travelling speed of the P wave, which is usually measured in-site and assumed to be a constant value in this study.

## 4. Micro-seismic event monitoring with in-situ records

### 4.1 Site conditions

The micro-seismic monitoring data used in this study were acquired from the Yongshaba mine in Kailin, Guizhou Province, China. The surface elevation of the phosphate mine is +1350 meters above the sea level, and the mining depth has reached to 700 m. The orebody is mainly brown phosphate rock, and the lithology is hard and compact. The density, tensile strength, uniaxial compressive strength, Young's modulus, Poisson's ratio, shear strength and internal friction angle are  $3.22 \text{ t/m}^3$ , 4.46 MPa, 147.89 MPa, 29.21 GPa, 0.25, 36.67 MPa, and  $41.94^\circ$ , respectively. The existence of more than twenty intensive faults and three dikes lead to the poor stability of Yongshaba mine, especially in the mining area under the Jin Yang highway, which is one of the

key areas for micro-seismic monitoring. Considering the engineering geology in the mining area, the in-situ conditions and the available budget and equipment, a digital micro-seismic monitoring system with 32 channels developed by Integrated Seismic System (ISS) Company in South Africa was installed in the mine. Institute of Mine Seismology (IMS) 14 Hz borehole geophones are used. They are omni-directional and can be installed at any angle, with a usable frequency bandwidth of between 8 Hz (-3dB point) and 2000 Hz and a small distortion less than 0.3%.

The sensor placement configuration in orebody is shown in Fig. 3, and the coordinates of sensors are given in Table 1. The World Geodetic System 84 (WGS84) is adopted in the sensor location measurement. The spatial coordinate system  $O$ -XYZ is defined with the origin of the coordinate system  $O$  located at the Earth's centre of mass. The coordinate axis  $X$  is along the intersecting lines of the first meridian plane and the surface of the equator taking the east as the positive direction. The  $Z$  axis corresponds to the rotation axis of the earth with the north taken as the positive direction. The  $Y$  axis is perpendicular to the  $XZ$  plane to build the right-handed system. The resolution of the coordinate system is 1m. The coordinates of the sensors in Table 1 are defined in the above coordinate system. In total, twenty-eight sensors have been installed in this area, marked as the red triangles with the sensor number as shown in Fig. 3. Two of them are tri-axial sensors, denoted as T1 and T2, and placed at over 700 m below the Yongshaba mine surface. The other twenty-six are single-axis sensors, which are numbered from 1 to 26, are evenly distributed in the three dikes #1, #2 and #3. The experimental data recorded by ten stable sensors, i.e., 1, 2, 3, 4, 8, 9, 12, 17, 18 and 22, are used to verify the proposed approach.

The identification of TDOA with recorded time histories from an individual micro-seismic event is conducted in section 4.2, and the statistical identification with measurements from multiple events is also performed in section 4.3 to analyse the robustness and reliability of the proposed approach.

Table 1 Coordinates of placed sensors in Yongshaba mine

Sensor No.	Location and coordinate	Sensor No.	Location and coordinate
T1	(381077.08,2996000.01 ,931.60)	T2	(381211.18,2996464.83,931.60)
1	(380971.24,2995790.77,931.60)	2	(381092.19,2996243.18,931.60)
3	(381299.97 ,2996630.72 ,931.60)	4	(381377.60 ,2996790.61 ,931.60)
5	(381447.91 ,2996915.33 ,931.60)	6	(381382.46 ,2997072.65 ,931.60)
7	(381317.12 ,2997244.78 ,931.60)	8	(381302.91 ,2997376.85 ,931.60)
9	(381277.24 ,2997590.28 ,931.60)	10	(381260.63 ,2997779.54 ,931.60)
11	(381612.53 ,2997810.08 ,1081.60)	12	(381606.62 ,2997647.03 ,1081.60)
13	(381684.58 ,2997460.55 ,1081.60)	14	(381621.00 ,2997310.74 ,1081.60)
15	(381690.19 ,2997074.72 ,1081.60)	16	(381573.54 ,2996951.43 ,1081.60)
17	(381472.07 ,2996783.25 ,1081.60)	18	(381400.84 ,2996632.61 ,1081.60)
19	(381369.99,2996436.86 ,1081.60)	20	(381398.59 ,2996275.20 ,1081.60)
21	(381305.20 ,2996087.08 ,1081.60)	22	(381274.89 ,2995856.38 ,1081.60)
23	(381732.06 ,2998077.64 ,1121.60)	24	(381707.72 ,2997975.13 ,1121.60)
25	(381685.80 ,2997859.31 ,1121.60)	26	(381701.09 ,2997716.63 ,1121.60)

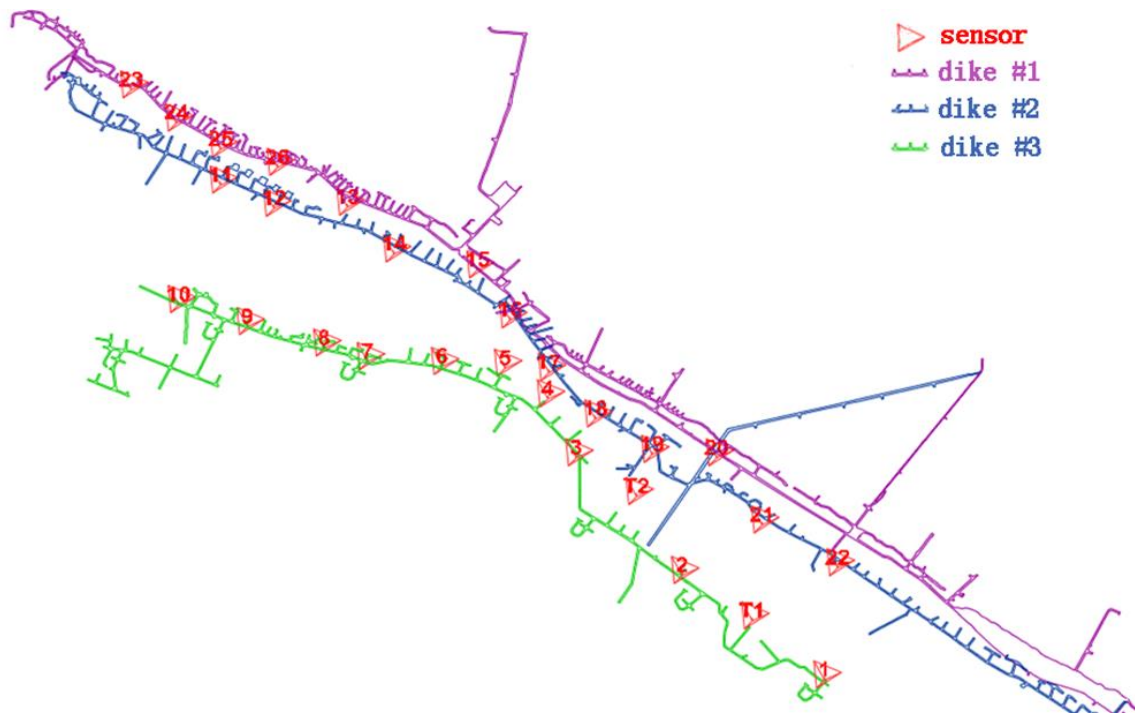


Fig. 3 The sensor placement configuration in Kailin phosphate mine

#### 4.2 Individual validation

As mentioned in Section 2, TDOA can also be estimated by the cross-correlation function based methods. Here, a case study is presented to compare the efficiency of the proposed approach with the cross-correlation function method, and demonstrate the superiority of the proposed approach against the noise effect in the recorded measurements. The cross-correlation method and the proposed approach are used separately with the same data, which are recorded from two sensors No. 1 and 12 under a micro-seismic event in the above-mentioned phosphate mine. The distance between sensors No.1 and No.12 is 1967.72 m, and the relative location of sensors No.12 to sensors No.1 is (635.38, 1856.26, 150.00). The sampling duration of those two signals is 1.5 s, and the sampling frequency is 6000 Hz. The measured waves from those two sensors are shown in Fig. 4.

The cross-correlation function of these two signals is calculated, and TDOA is obtained by identifying the time offset corresponding to the maxima in the cross-correlation function. As shown in Fig. 5(a), TDOA is identified as 0.166 s when using the original signals without artificially added white noise. However, as shown several peaks exist in the cross-correlation function, indicating that a tiny time offset may induce a significant change in the cross-correlation, which also means this method is susceptible to noise. When an extra 10 db white noise is added to the original signals, the local maximum point becomes the global maximum point and TDOA is identified as 0.203 s, as shown in Fig. 5(b). This demonstrates that the noise has a significant effect on the identification accuracy of TDOA when using cross-correlation method.

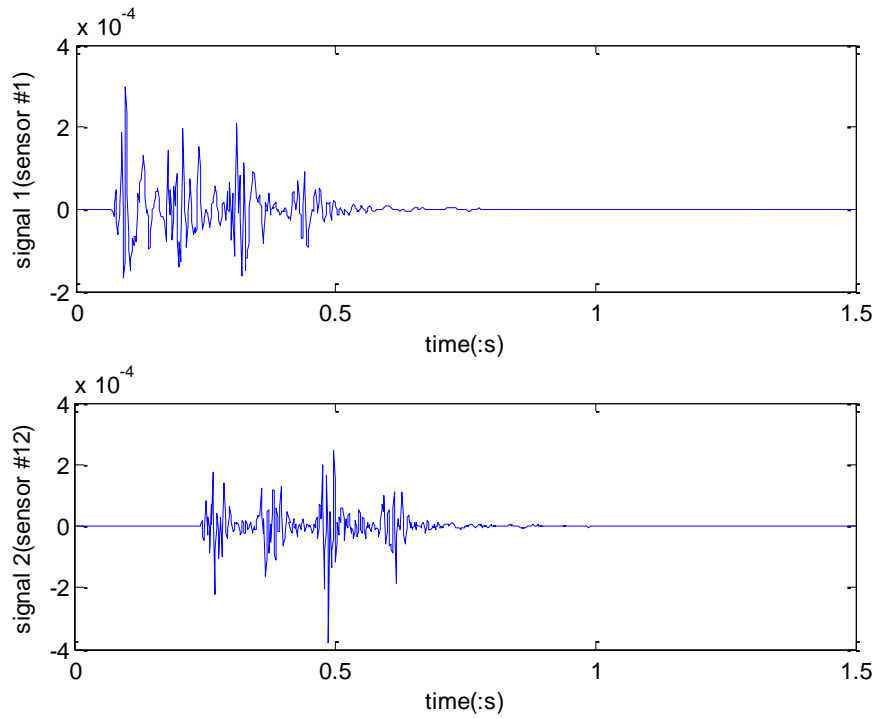


Fig. 4 Original signals measured in a real micro-seismic event by sensors No.1 and No.12

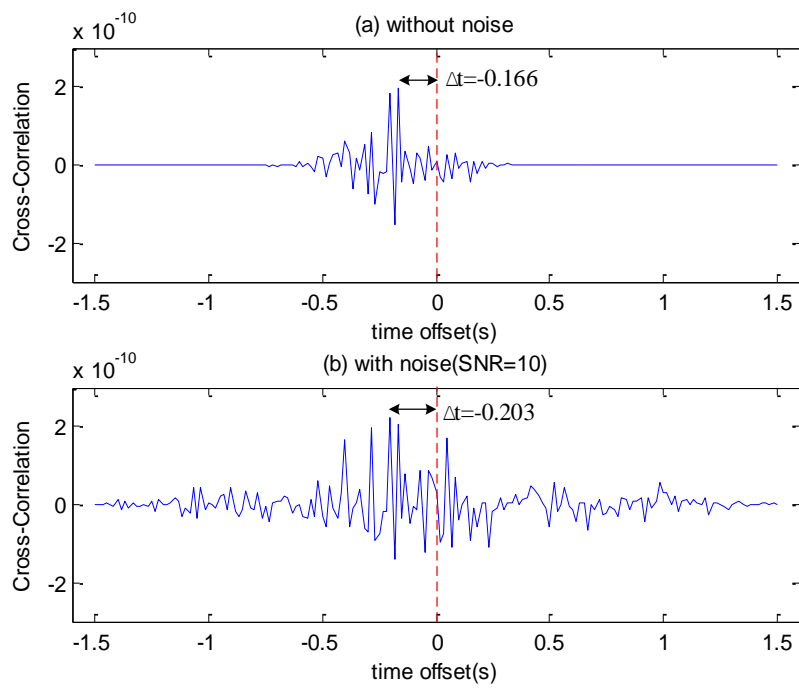


Fig. 5 Cross-correlation function of measured signals: (a) without noise effect (b) with 10 dB artificial white noise

Meanwhile the proposed approach based on cross wavelet transform is used to analyse the above signals. The merits of wavelet transform are to capture the multi-scale information and reflect the signal characteristics in both the time and frequency scales. Then a specific frequency range is used for the identification as a filter function, and the time offset according to the maximum power of the cross wavelet transform spectrum would indicate the estimation of TDOA. It should be noted that a frequency band with the cut-off frequency of 2 Hz and 256 Hz are used in the calculation for the sake of removing the high-frequency noise components. These cut-off frequencies sufficiently cover the frequency range of the micro-seismic signals, which is usually in the band from 50-200 Hz (Li *et al.* 2008, Lu *et al.* 2008).

The original signals and the corresponding continuous wavelet transform spectrum are shown in Fig. 6. It should be noted that the thick black contour designates the 5% significance level against the red noise, and the COI where edge effects might distort the spectrum is shown as a

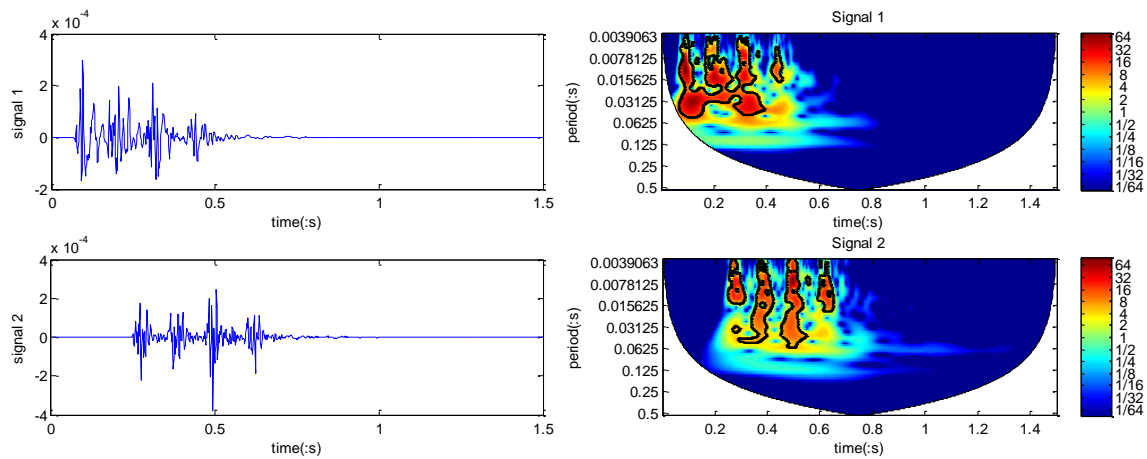


Fig. 6 The original signals and their continuous wavelet power spectrum

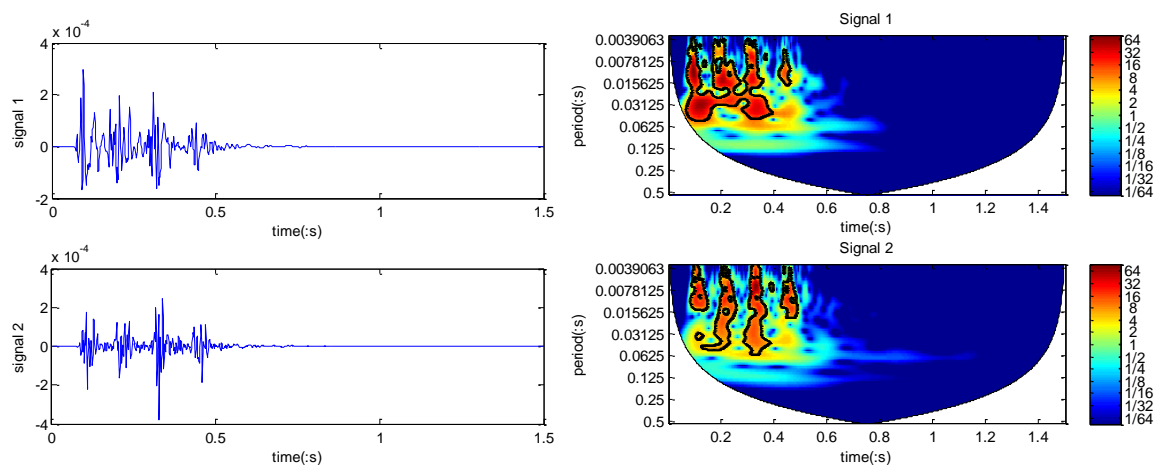


Fig. 7 The shifted signals and their continuous wavelet power spectrum

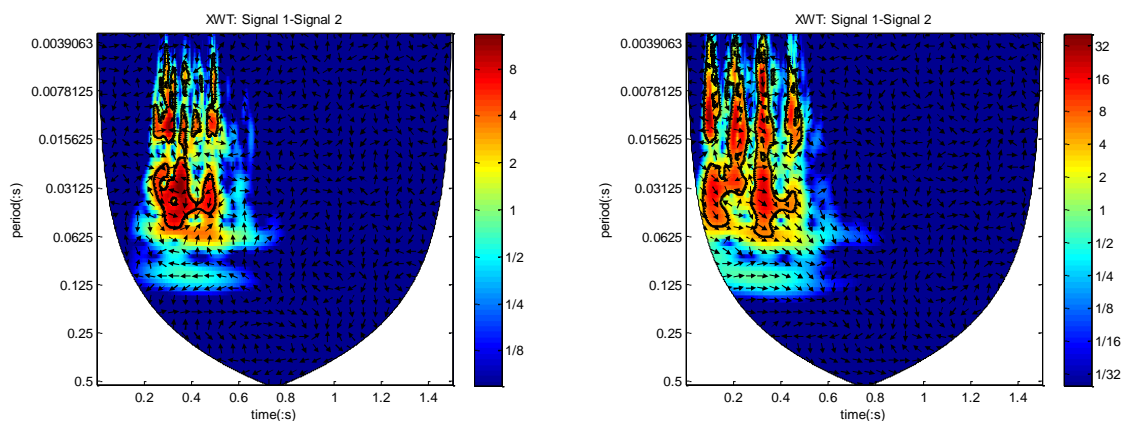
lighter shade. The 5% significance level and COI are applied in computing the wavelet transform spectrum to improve the edge effect.

When the first signal is delayed by 0.166 s, the shifted signals and their associated continuous wavelet transform spectrum are shown in Fig. 7. It can be observed that the region with a larger energy in the wavelet transform spectrum is also moved with the delay.

Similar to the idea of using cross-correlation function to identify TDOA, the cross wavelet transform power is calculated here. The offset time instant corresponding to the maximum cross wavelet spectrum power is detected as TDOA, and the location of the micro-seismic event is determined with three TDOAs. The cross wavelet transforms between those two original and shifted signals as shown in Fig. 6 and Fig. 7 are computed, and their spectrums are shown in Fig. 8(a) and Fig. 8(b), respectively. Comparing the energy intensities as shown in Fig. 8(a) and Fig. 8(b), the total cross wavelet spectrum power decreases significantly, indicating those two signals with an added delay are losing their similarity and having a worse correlation.

It is worth noting that the closer the delay of the two signals to the true TDOA, the larger the power of cross wavelet spectrum. This shows that the cross wavelet spectrum power would be an alternative good index to evaluate the similarity of two recorded signals and identify TDOA. One special merit of the wavelet analysis is keeping both the time and frequency information. Therefore, a better estimation of TDOA can be obtained in the micro-seismic monitoring.

The proposed approach is applied to analyse the signals in Fig. 4. The curve of the cross wavelet spectrum power with 95% significance level under different time offsets is shown in Fig. 9. When the originally recorded signals are analysed, the detection result is shown in Fig. 9(a). One obvious peak is found, and TDOA is identified as 0.166 s, which is exactly equal to the identified value from the cross-correlation method as shown in Fig. 5(a). When an extra artificial 10dB white noise is added to the recorded signals, the cross wavelet spectrum power is still smooth, and only one obvious peak is observed. TDOA is also identified as 0.166s, which is the same as that identified with original signals. These results demonstrate that the proposed method is less influenced by noise effect in identifying the TDOA compared with the existing cross-correlation method.



(a) Cross wavelet transform of two original signals as shown in Fig. 6

(b) Cross wavelet spectrum of two shifted signals as shown in Fig. 7

Fig. 8 Comparison of cross wavelet transform spectrum with the original and shifted signals

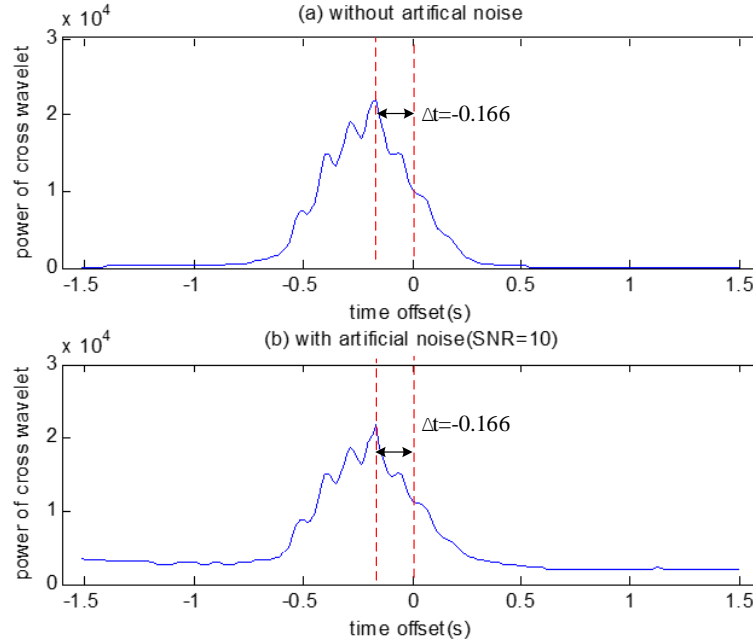


Fig. 9 Cross wavelet transform spectrum power: (a) using original signals (b) using signals smeared with 10dB white noised

Furthermore, the event source is located by the recorded signals from sensors No. 1, 12, 22 and the calculated TDOA among those three sensor locations. Reference TDOA value defined in this study is picked manually by an independent experienced analyst and the reference location is calculated with Eq. (2) and the Quasi-Newton method. It should be noted that the determined micro-seismic location might not be the exactly real location of the event. However, this is the general practice to define the baseline TDOA and location (Saragiotis *et al.* 2004). Those TDOA and subsequently obtained location will be used as the reference for comparing the performance of different methods in this paper.

The cross-correlation method and the proposed approach are used respectively to process the data and identify the source location for comparison. The reference values of TDOA, identified values with the cross-correlation method and the proposed approach, and the identified event source location are given in Table 2. The P-wave speed in the site was measured as 5349.47 m/s. When taking the calculated source location with reference TDOA values as the baseline coordinates of the source event, noted as  $(x_r, y_r, z_r)$ , the absolute location error is defined as

$$\text{Absolute location error} = \sqrt{(x_i - x_r)^2 + (y_i - y_r)^2 + (z_i - z_r)^2} \quad (19)$$

where  $(x_i, y_i, z_i)$  are the spatial coordinates of the identified source location. The absolute locating error of the proposed approach is calculated as 8.9 m, while the error of the cross-correlation method is 172.5 m. This demonstrates that the proposed approach significantly improves the identification accuracy for the micro-seismic event monitoring and source locating with the in-situ measured records from an individual event.

Table 2 TDOA obtained by cross-correlation method and the proposed approach in an individual test

Sensors No.	Reference	Cross-correlation	The proposed approach
1 & 12	-166 ms	-203 ms	-166 ms
1 & 18	45 ms	58 ms	47 ms
12 & 22	-26 ms	-17 ms	-25 ms
Identified source location	(380949.5, 2996534.7, 875.9)	(381060.9, 2996595.7, 992.6)	(380955.1, 2996535.2, 882.8)

Besides the above example to demonstrate the accuracy and performance of the proposed approach against the noise effect, the statistical verification will be performed with recorded in-field data from multiple micro-seismic events.

#### 4.3 Statistical verification

In this section, recorded data from ten sensors, namely No. 1, 2, 3, 4, 8, 9, 12, 17, 18, and 22, under five real micro-seismic events are analysed. Any two of those ten sensors could be used to identify a TDOA, therefore forty-five TDOAs can be obtained under an event. For five separate micro-seismic events, two hundred and twenty-five TDOAs will be obtained totally and used for investigating the statistical identification accuracy with the proposed approach and those existing methods presented in Section 2, i.e., cross-correlation method, multi-correlation method, STA/LTA method and Kurtosis method. When defining the parameters for these methods, the number of samples of the long term windows  $N_{LTA}$  and the short term windows  $N_{STA}$  are assigned as 1000 and 500 samples respectively in STA/LTA method. The length of the sliding window  $N$  is set as 200 samples for Kurtosis method.

The difference between the identified TDOA  $\tau_{identified}$  and the reference TDOA  $\tau_{ref}$  is defined as the absolute identification error as follows

$$\text{Absolute error in TDOA} = |\tau_{identified} - \tau_{ref}| \quad (20)$$

The mean value and standard deviation of the absolute identification errors are calculated. For a sequence  $e_{i(i=1, \dots, N)}$ , the mean value and standard deviation are respectively calculated as

$$\mu = \frac{1}{N} \sum_{i=1}^N e_i \quad (21)$$

$$S = \sqrt{\frac{\sum_{i=1}^N (e_i - \mu)^2}{N - 1}} \quad (22)$$

The statistical results of absolute errors of TDOA with different approaches are listed in Table 3. The mean value and standard deviation by the four existing methods and the proposed approach are listed, which are marked as A (Cross-correlation method), B (Multi-correlation method), C (STA/LTA method), D (Kurtosis method) and E (The proposed approach). Four additional artificial noise levels with Signal to Noise Ratio (SNR)=infinite (i.e., no noise effect), 20 dB, 10 dB and 5 dB are considered. For noisy cases, the extra noise effect is added on the originally



recorded data to further verify the robustness of the proposed approach.

Results in Table 3 demonstrate that the proposed approach gives the smallest mean value and standard deviation of the identification errors among all the five methods. The results also clearly show that the proposed approach is less sensitive to noise effect than the other four existing methods. Fig. 10 shows the box plot of the error analysis results. The bottom and top of the box denote the first and third quartiles, respectively, and the band inside the box denotes the mean value. The two ends of the dashed line represent the minimum and the maximum values of the absolute error. As shown in Fig. 10, the error of identification results with the four existing approaches, namely A, B, C and D, are obviously increasing with the severity of noise, indicating those methods are significantly affected by noise effect. The Kurtosis method is the most sensitive to the noise and then the Cross-correlation method. STA/LTA and the multiple-correlation

Table 3 Statistical results of absolute errors (unit: ms) of TDOA under different artificial noise level

Method	SNR Items	+inf (No artificial noise)	20 dB	10 dB	5 dB
Cross-correlation (A)	Mean	3.2	3.7	5.7	12.8
	standard deviation	5.6	6.5	7.3	18.5
Multi-correlation (B)	Mean	2.4	3.7	5.1	11.6
	standard deviation	4.4	4.6	6.6	15.9
STA/LTA (C)	Mean	5.9	6.2	9.4	14.8
	standard deviation	8.2	12.5	16.1	23.3
Kurtosis (D)	Mean	3.1	5.7	8.5	14.3
	standard deviation	6.2	7.5	12.1	31.5
The proposed approach (E)	Mean	1.5	2.1	1.9	2.1
	standard deviation	2.1	2.7	3.2	3.4

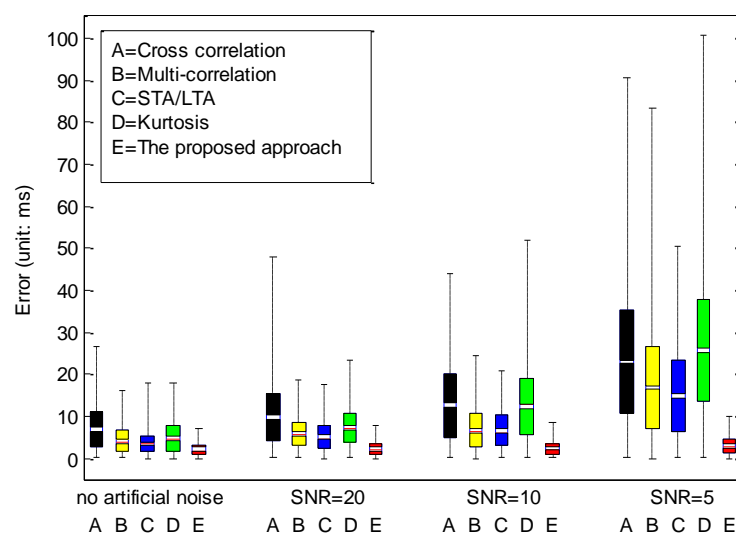


Fig. 10 Errors in TDOA of statistical identification results with different approaches

methods have the similar performance to the influence of noise effect. The proposed approach is also affected by the noise in recorded signals, but at a less extent, indicating it is more robust compared with the other four existing methods.

Furthermore, the locations of five micro-seismic events are identified to demonstrate the accuracy of the proposed approach in micro-seismic event source locating. For every single seismic event, any four sensors selected from the above mentioned ten sensors can be used to identify the event location. Different combinations with three sensors from those ten sensors will give different identification results. Therefore 210 location results can be obtained for each event. Approaches A, B, C, D and E are used to calculate the source location respectively, and the standard deviation of the predicted absolute source locations is given in Table 4.

For one event, the locations computed by different sensor combinations are  $(x_i, y_i, z_i)$  ( $i=1, \dots, 210$ ), then the centre point  $(\bar{x}, \bar{y}, \bar{z})$  can be calculated by

$$\begin{aligned}\bar{x} &= \frac{\sum_{i=1}^N x_i}{N} \\ \bar{y} &= \frac{\sum_{i=1}^N y_i}{N} \\ \bar{z} &= \frac{\sum_{i=1}^N z_i}{N}\end{aligned}\quad (23)$$

In Table 4, the STD is the standard deviation (see equation (22)) of  $d_i$ , where  $d_i$  is

$$d_i = \sqrt{(x_i - \bar{x})^2 + (y_i - \bar{y})^2 + (z_i - \bar{z})^2} \quad (24)$$

It can be observed from Table 4 that the standard deviation of the proposed approach is the smallest among all the methods, which indicates that the proposed method is more accurate and reliable with a small variation in the predicted source locations.

In addition to investigating the robustness and reliability of the existing methods and the proposed approach, the error analysis on the identification results of the source locations is also conducted. Eq. (19) is used to calculate the identification error of the source location. The statistical results of identification errors of the source locations are shown in Table 5 and Fig. 11. It can be observed that the proposed approach significantly outperforms the other four existing methods on the identification accuracy of source location of the micro-seismic events with a much smaller mean error and standard deviation.

As shown in Fig. 11, the proposed approach gives the best estimation of the locations of those five micro-seismic events. The medium and maximum location error is the smallest compared with the other methods. It also shows a stable performance compared with the other four methods since the observed Quartile Deviation (the difference of the first quartile value and the third quartile value) of the location error is insignificant.

Table 4 The standard deviation (unit: m) of identified source locations

	Event 1	Event 2	Event 3	Event 4	Event 5
A	26.88	29.39	17.12	22.85	17.60
B	10.76	11.56	19.92	18.58	12.13
C	17.99	15.17	16.01	15.27	12.93
D	16.07	17.39	15.62	12.05	13.29
E	5.39	6.23	14.02	5.76	9.90

Table 5 Absolute errors (unit: m) of micro-seismic event location in the statistical identification results

Method	Event ID Items	Event 1	Event 2	Event 3	Event 4	Event 5
A	mean	55.16	28.76	33.28	43.15	53.50
	standard deviation	66.28	38.14	23.67	32.43	51.71
B	mean	26.79	16.25	20.81	26.41	21.89
	standard deviation	25.46	11.02	27.52	33.26	24.31
C	mean	28.91	11.89	26.45	18.71	16.98
	standard deviation	26.25	22.65	13.82	31.16	13.16
D	mean	26.41	18.34	28.97	29.68	31.62
	standard deviation	23.27	18.91	21.06	21.29	38.66
E	mean	8.03	5.68	11.21	15.62	14.39
	standard deviation	16.57	9.39	14.32	20.23	10.07

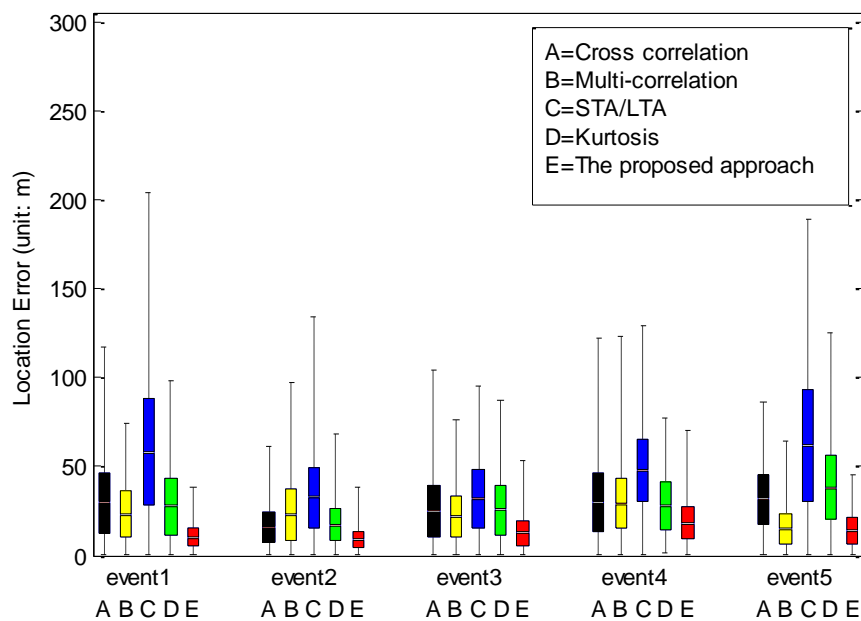


Fig. 11 Errors in event location of statistical identification results with different approaches

The above verification results demonstrate the proposed method is much less sensitive to the noise effect, more reliable and robust than the other existing automatic picking methods. The effectiveness and superiority of the proposed approach in micro-seismic monitoring is well proved.

## 5. Conclusions

This paper proposes a new micro-seismic monitoring approach based on cross wavelet

transform. The proposed approach transforms time series into time-frequency domain and can achieve multi-scale analysis for a better identification of TDOA by cross wavelet transform and spectral analysis. The theoretical background of several typical methods to identify TDOA is reviewed, and the main idea and flowchart of the proposed approach are presented. The cross wavelet transform is utilized to analyse the measured signals under micro-seismic events, and the cross wavelet power spectrum is used to measure the similarity of two signals in a multi-scale dimension and subsequently identify TDOA. The offset time instant corresponding to the maximum cross wavelet transform spectrum power is identified as TDOA, and then the location of micro-seismic events can be identified. Individual and statistical verifications are performed with recorded data from a mine in China. The results demonstrate that the proposed method gives more accurate identification of micro-seismic location, and is less sensitive to noise effect, as compared to the four other existing methods.

It is the first time that cross wavelet transform spectrum is used to identify TDOA and then to locate the micro-seismic event. It not only preserves the advantage of traditional relative methods by avoiding the errors introduced by manually picking up the first arrival wave, but also utilizes the advantages of wavelet analysis methods, which provides a time-frequency multi-scale analysis. It has both frequency resolution and time resolution, which is of vital importance to analyse the nonstationary signals. Analysis results with in-situ measurement records demonstrate that the proposed approach outperforms other methods with a more accurate and reliable micro-seismic event location identification result.

## Acknowledgements

The first author thanks the partial support of projects (11472311, 41272304, and 51504288) of the National Natural Science Foundation of China

## References

- Aminzadeh, F., Maity, D., Tafti, T.A. and Brouwer, F. (2011), "Artificial neural network based autopicker for micro-earthquake data", *2011 SEG Annual Meeting*, San Antonio, Texas, September.
- Boschetti, F., Dentith, M. and List, R. (1996), "A fractal-based algorithm for detecting first arrivals", *Geophysics*, **61**(4), 1095-1102.
- Carter, G.C. (1987), "Coherence and time delay estimation", *Proc. IEEE*, **75**(2), 236-255.
- Chalmers, D.R. (2013), "Explosions in mines-systematic failure", *23rd World Mining Congress 2013 Proceedings*, Montreal, Canada, August.
- Correig, A.M. and Urquizú, M. (2002), "Some dynamical characteristics of microseism time-series", *Geophys. J. Int.*, **149**(3), 589-598.
- Dong, L.J., Li, X.B. and Xie, G.N. (2014), "Nonlinear methodologies for identifying seismic event and nuclear explosion using random forest, support vector machine, and naive bayes classification", *Abstract Appl. Anal.*, **2014**(1), 1-8.
- Earle, P.S. and Shearer, P.M. (1994), "Characterization of global seismograms using an automatic-picking algorithm", *Bull. Seismol. Soc. Am.*, **84**(2), 366-376.
- Gomberg, J.S., Shedlock, K.M. and Roecker, S.W. (1990), "The effect of S-wave arrival times on the accuracy of hypocenter estimation", *Bull. Seismol. Soc. Am.*, **80**(6A), 1605-1628.
- Grinsted, A., Moore, J.C. and Jevrejeva, S. (2004), "Application of the cross wavelet transform and wavelet coherence to geophysical time series", *Nonlin. Proc. Geophys.*, **11**(5/6), 561-566.

- Han, L., Wong, J. and Bancroft, J. (2010), "Time picking on noisy microseismograms", *Proceedings of the GeoCanada 2010 Convention-Working with the Earth*, Calgary, AB, Canada.
- He, X.L. and Zhao, L.Z. (2010), "Analysis of shear wave velocity based on multiple cross-correlation functions", *Rock Soil Mech.*, **31**(8), 2541-2545. (In Chinese)
- Huang, Y.A. and Benesty, J. (Eds.) (2007), *Audio signal processing for next-generation multimedia communication systems*, Springer Science & Business Media, 197-253.
- Jiang, F., Kuang, Y. and Astrom, K. (2013), "Time delay estimation for TDOA self-calibration using truncated nuclear norm regularization", *IEEE International Conference on Acoustics, Speech and Signal Processing*, Vancouver, BC, May.
- Jiao, L. and Moon, W.M. (2012). "Detection of seismic refraction signals using a variance fractal dimension technique", *Geophysics*, **65**(1), 286-292.
- Knapp, C.H. and Carter G.C. (1976), "The generalized correlation method for estimation of time delay", *IEEE Trans. Acoust., Speech, Sign. Proc.*, **24**(4), 320-327.
- Kwon, O.Y. and Chan, J.Y. (1998), "Source location in plate by using wavelet transform of AE signals", *14th International AE Symposium & 5th AE World Meeting (Vol. 4)*, Hawaii, USA, August.
- Kwon, B., Park, Y. and Park, Y. (2010), "Analysis of the GCC-PHAT technique for multiple sources", *2010 International Conference on Control Automation and Systems*, Gyeonggi-do, October.
- Li, J., Hao, H., Xia, Y. and Zhu, H.P. (2015a), "Damage assessment of shear connectors with vibration measurements and power spectral density transmissibility", *Struct. Eng. Mech.*, **54**(2), 257-289.
- Li, J., Hao, H. and Lo, J.V. (2015b), "Structural damage identification with power spectral density transmissibility: numerical and experimental studies", *Smart Struct. Syst.*, **15**(1), 15-40.
- Li, J. and Hao, H. (2016), "A review of recent research advances on structural health monitoring in Western Australia", *Struct. Monit. Mainten.*, **3**(1), 33-49.
- Law, S.S., Zhu, X.Q., Tian, Y.J., Li, X.Y. and Wu, S.Q. (2013), "Statistical damage classification method based on wavelet packet analysis", *Struct. Eng. Mech.*, **46**(4), 459-486.
- Li, Z.M., Gou, X.M., Jin, W.D., Qin, N., Liu, J.B. and Luo, X. (2008), "Frequency feature of microseismic signals", *Chinese J. Geophys. Eng.*, **30**(6), 830-834. (In Chinese)
- Liu, W.D., Zhang, W. and Dou, L.M. (2009), "Research of the time difference computation in acoustic emission location", *Comput. Eng. Sci.*, **31**(4), 127-129. (In Chinese)
- Lu, C.P., Dou, L.M., Cao, A.Y. and Wu, X.R. (2008), "Research on microseismic activity rules in Sanhejian coal mine", *J. Coal Sci. Eng. (China)*, **14**(3), 373-377.
- McCormack, M., Zuchta, D. and Dushek, D. (1993), "First-break refraction event picking and seismic data trace editing using neural networks", *Geophysics*, **58**(1), 67-78.
- Munro, K.A. (2004), "Automatic event detection and picking P-wave arrivals", *CREWES Research Report*, **16**(12), 1-10.
- Nistor, S. and Buda, A.S. (2015), "Ambiguity resolution in precise point positioning technique: a case study", *J. Appl. Eng. Sci.*, **5**(1), 53-60.
- Pavlis, G.L. (1986), "Appraising earthquake hypocenter location errors: a complete, practical approach for single-event locations", *Bull. Seismol. Soc. Am.*, **76**(6), 1699-1717.
- Saragiotis, C.D., Hadjileontiadis, L.J. and Panas, S.M. (2002), "PAI-S/K: a robust automatic seismic P phase arrival identification scheme", *IEEE Trans. Geosci. Remote Sens.*, **40**(6), 1395-1404.
- Sobolev, G.A., Lyubushin, A.A. and Zakrzhevskaya, N.A. (2005), "Synchronization of microseismic variations within a minute range of periods", *Izvestiia Physics of the Solid Earth C/C Of Fizika Zemli-Rossiiskaia Akademiia Nauk*, **41**(8), 599-621.
- Saragiotis, C.D., Hadjileontiadis, L.J., Rekanos, I.T. and Panas, S.M. (2004), "Automatic P phase picking using maximum kurtosis and  $\kappa$ -statistics criteria", *IEEE Geosci. Remote Sens. Lett.*, **1**(3), 147-151.
- Waldhauser, F. and Ellsworth, W.L. (2000), "A double-difference earthquake location algorithm: method and application to the northern hayward fault, California", *Bull. Seismol. Soc. Am.*, **90**(6), 1353-1368.
- Wang, Q. and Chu, F. (2001), "Experimental determination of the rubbing location by means of acoustic emission and wavelet transform", *J. Sound Vib.*, **248**(1), 91-103.
- Wong, J., Han, L., Bancroft, J. and Stewart, R. (2009), "Automatic time-picking of first arrivals on noisy

- microseismic data”, CSEG. 0 0.2 0.4 0.6 0.8 1.1.2, 1-4.
- Xing, H.Y., Liu, Z.Q. and Wan, M.X. (2002), “The generalized correlation algorithm for estimation of time delay based on wavelet transform”, *ACTA Acustica*, **27**(1), 88-93. (In Chinese)
- Yuksel, S.B. and Yazar, A. (2015), “Neuro-fuzzy and artificial neural networks modeling of uniform temperature effects of symmetric parabolic haunched beams”, *Struct. Eng. Mech.*, **56**(5), 787-796.
- Zhang, H.L., Zhu, G.M. and Wang, Y.H. (2013), “Automatic microseismic event detection and picking method”, *Geophys. Geochem. Explor.*, **37**(2), 269-273. (In Chinese)
- Zhong, S., Xia, W., He, Z., Hu, J. and Li, J. (2014), “Time delay estimation in the presence of clock frequency error”, *2014 IEEE International Conference on Acoustics, Speech and Signal Processing*, Florence, Italy, May.
- Zhao, C. (2015), “Analytical solutions for crack initiation on floor-strata interface during mining”, *Geomech. Eng.*, **8**(2), 237-255.